Published OnlineFirst November 6, 2013; DOI: 10.1158/1541-7786.MCR-13-0164

Oncogenes and Tumor Suppressors

Molecular Cancer Research

C-C Chemokine Receptor 5 on Pulmonary Mesenchymal Cells Promotes Experimental Metastasis via the Induction of Erythroid Differentiation Regulator 1

Robert L. Mango[1], Qing Ping Wu[3], Michelle West[3], Everett C. McCook[3], Jonathan S. Serody[1,2,3], and Hendrik W. van Deventer[2]

Abstract

C-C Chemokine receptor 5 knockout ($Ccr5^{-/-}$) mice develop fewer experimental pulmonary metastases than wild-type (WT) mice. This phenomenon was explored by applying gene expression profiling to the lungs of mice with these metastases. Consequently, erythroid differentiation regulator 1 (*Erdr1*) was identified as upregulated in the WT mice. Though commonly associated with bone marrow stroma, *Erdr1* was differentially expressed in WT pulmonary mesenchymal cells (PMC) and murine embryonic fibroblasts (MEF). Moreover, the Ccr5 ligand Ccl4 increased its expression by 3.36 ± 0.14–fold. Ccr5 signaling was dependent on the mitogen-activated protein kinase kinase (Map2k) but not the phosphoinositide 3-kinase (Pi3k) pathway because treatment with U0126 inhibited upregulation of *Erdr1*, but treatment with LY294002 increased the expression by 3.44 ± 0.92–fold ($P < 0.05$). The effect *Erdr1* on B16-F10 melanoma metastasis was verified by the adoptive transfer of WT MEFs into $Ccr5^{-/-}$ mice. In this model, MEFs that had been transduced with *Erdr1* short hairpin RNA (shRNA) lowered metastasis by 33% compared with control transduced MEFs. The relevance of ERDR1 on human disease was assessed by coculturing chronic lymphocytic leukemia (CLL) cells with M2-10B4 stromal cells that had been transfected with shRNA or control plasmids. After 96 hours of coculture, the cell counts were higher with control cell lines than with *Erdr1* knockdown lines [odds ratio (OR), 1.88 ± 0.27, 2.52 ± 0.66, respectively]. This increase was associated with a decrease in apoptotic cells (OR, 0.69 ± 0.18, 0.58 ± 0.12, respectively).

Implications: Therefore, ERDR1 is a stromal-derived factor that promotes cancer cell survival *in vitro* and in an experimental metastasis model. *Mol Cancer Res; 12(2); 274–82. ©2013 AACR.*

Introduction

Over the past 10 years, evidence has emerged highlighting the importance of stromal cells in cancer progression (1–4). During metastasis, the associated stroma is remodeled by the activation of fibroblasts and the recruitment of bone marrow–derived cells. Although the mediators of this process continue to be elucidated, several are well established, including platelet-derived growth factor receptor (PDGFR) ligands (5), matrix metalloproteinase 9 (MMP9) (6), interleukin 6 (IL6) (7), S100A4, and S100A8 (8, 9). These mediators are of clinical importance because they provide therapeutic targets, which may be critical for the treatment of chemotherapy-resistant tumors.

Authors' Affiliations: [1]Departments of Microbiology and Immunology and [2]Medicine; and [3]Lineberger Comprehensive Cancer Center, University of North Carolina, Chapel Hill, North Carolina

Note: Supplementary data for this article are available at Molecular Cancer Research Online (http://mcr.aacrjournals.org/).

Corresponding Author: Hendrik van Deventer, University of North Carolina, CB 7305, 170 Manning Drive, Chapel Hill, NC 27599-7305. Phone: 919-966-4431; Fax: 919-966-8212; E-mail: hvand@med.unc.edu

doi: 10.1158/1541-7786.MCR-13-0164

We have previously shown that stromal cells expressing Ccr5 contribute to the formation of a metastasis-promoting stroma. Specifically, the activation of Ccr5 on pulmonary mesenchymal cells (PMC) leads to the induction of Mmp-9 (10). These results have been extended by others studying the Ccr5 ligand Ccl3. In addition to Mmp9, tumors in $Ccr5^{-/-}$ and $Ccl3^{-/-}$ mice produce less hepatocyte growth factor and accumulate fewer monocytes and T cells than tumors in wild-type (WT) mice (11). Ccr5 expression by the host also contributes to the survival of cancer cells by inhibiting apoptosis (12).

Given the importance of CCR5, we decided to further investigate this mechanism by comparing gene expression in WT versus $Ccr5^{-/-}$ lungs after the injection of B16-F10 melanoma cells. These experiments led to our characterization of the gene *erythroid differentiation regulator 1* (*Erdr1*) as a metastasis-promoting signal.

ERDR1 was first isolated from the myelomonocytic cell line WEHI-3B as a cytokine that induced hemoglobin synthesis (13). However, a wider biologic function was suggested by its expression in other cell types, including murine fibroblasts, lymphoma cells, and human peripheral blood mononuclear cells (14). In addition to hemoglobin synthesis, ERDR1 also acts as a survival signal during periods of cellular stress. This

Published OnlineFirst November 6, 2013; DOI: 10.1158/1541-7786.MCR-13-0164

function has been established in erythroblasts, granulocyte/monocyte progenitors, and hematopoietic stem cells (14). A greater significance of this gene is also implied by its differential expression on a number of cDNA microarrays, including those analyzing brain inflammation, neurodegeneration (15–17), and development (18, 19).

In this report, we show that ERDR1-expressing stroma promotes cancer cell survival *in vitro* and during cancer cell invasion. Furthermore, the gene is upregulated by chemokine ligand binding to CCR5. Therefore, ERDR1 may be an innovative therapeutic target either directly or indirectly by inhibiting CCR5.

Materials and Methods

Mice

C57BL/6J (WT) mice were purchased from The Jackson Laboratories. The generation of B6.129P2-*Ccr5*^{tm1Kuz}/J (*Ccr5*$^{-/-}$) mice has been described previously (20). Males and females between 8 and 12 weeks were used in these experiments. Controls and experimental groups were balanced by age and gender. All animals were housed in pathogen-free conditions and all experiments were conducted using protocols approved by the Institutional Animal Care and Use Committee of the University of North Carolina (Chapel Hill, NC).

Cells

B16-F10 melanoma, A293T, and M2-10B4 cells were purchased from American Type Culture Collection. Upon receipt, these cells were expanded by three to four passages and were frozen into aliquots to maintain their uniformity and veracity. B16-F10 cells were additionally verified by melanin production. Aliquots were passaged twice after thawing and before use.

Isolation of PMCs was performed as previously described (10). In all experiments, PMCs were used within two passages of isolation. Murine embryonic fibroblasts (MEF) were harvested from embryonic day 13.5 embryos as described elsewhere (21) and were transduced after two to five *ex vivo* passages.

All murine cell types were cultured in Dulbecco's Modified Eagle Medium (DMEM) supplemented with 10% FBS and 1% penicillin/streptomycin (Gibco). Human chronic lymphocytic leukemia (CLL) cells were cultured in complete RPMI (Gibco) with 10% FBS.

Flow cytometry and cell sorting

Identification of PMC populations was accomplished by incubating the cells with anti-Thy-1.2-PECy7 (eBioscience) and anti-CD45-eFluor450 (eBioscience) antibodies for 15 minutes at room temperature. CD45$^+$ cells were sorted by the UNC Flow Cytometry Facility. Apoptotic cells were identified by staining the cells with propidium iodide (PI) and Annexin V–allophycocyanin (eBioscience) for 15 minutes at room temperature. Fluorescence was measured on the MACSQuant Analyzer (Miltenyi) and was analyzed using the Summit software (Beckman Coulter).

In vitro experiments

PMCs were maintained overnight in serum-free conditions before chemokine treatment. The following day, 50 ng/mL of Ccl4 (Peprotech Inc.) was added. mRNA was harvested 24 and 48 hours after stimulation. Intracellular signaling pathways were investigated by adding 10 μmol/L of the mitogen-activated protein 2 kinase (MAP2K) inhibitor U0129 or 20 μmol/L of the phosphoinositide 3-kinase (PI3K) inhibitor LY294002 (Cell Signaling Technology). Both inhibitors were reconstituted in dimethyl sulfoxide (DMSO) before being diluted with media. Control wells were treated with media containing equivalent amounts of DMSO.

Apoptosis was induced with staurosporine treatment. For these experiments, MEFs were seeded onto 6-well plates 48 hours after transduction. After resting overnight, the cells were incubated with 100 nmol/L staurosporine plus 20 μmol/L Z-VAD-FMK (inhibitor) or Z-FA-FMK (control peptide; Sigma-Aldrich). Apoptosis was measured 24 hours later using Annexin V and PI as described above.

In vivo experiments

Cell transfer experiments were performed by tail vein injection in a total volume of 200μL of PBS. 4×10^5 MEFs were injected followed by 7.5×10^5 B16-F10 cells. The mice were given 48 hours rest between injections. Fourteen days after melanoma injection, the lungs were harvested and insufflated with the Fekete solution. Lung metastatic nodules were counted by an individual blinded to the experimental group (10).

Enhanced green fluorescent protein (eGFP) expression by cells within the lung was measured using an eGFP ELISA (Cell BioLabs). To do so, the left upper lobe of the lung was harvested after perfusing the animal with PBS. These samples were then homogenized in the presence of PBS and a protease-inhibitor cocktail (Roche). Supernatants were added to the ELISA plate following two centrifugation steps. The plates were then processed according to the manufacturer's instructions.

RNA analysis

Gene array experiments were performed on the lungs of WT and *Ccr5* $^{-/-}$ mice. These lungs were harvested at 6, 24, and 48 hours after intravenous injection with 7.5×10^5 B16-F10 melanoma cells. Passenger leukocytes were removed by perfusing the mice with PBS warmed to 37°C. The samples were flash-frozen and stored in liquid nitrogen before processing. mRNA isolation and cDNA formation have been previously described (10). The resulting cDNA was normalized by amount, pooled by time point, and hybridized to Affymetrix GeneChip Genome 430 Arrays (six arrays in total; Affymetrix). Gene expression was analyzed using the GeneSpring software (Agilent Technologies). All microarray data are minimum information about a microarray experiment (MIAME) compliant and have been deposited at Geo Expression Omnibus (GEO) (GEO ID: GSE51422). Confirmation of the microarray studies was performed by semiquantitative

Published OnlineFirst November 6, 2013; DOI: 10.1158/1541-7786.MCR-13-0164

real-time PCR (RT-PCR) as previously described (10). See Supplementary Experimental Procedures for primer sequences.

PMC or MEF mRNA was amplified by RT-PCR using the reagents and primers given in the Supplementary Experimental Procedures. RT-PCR was performed using SYBR Green Master Mix (Applied Biosystems). For analysis of PMC or MEFs, *Erdr1* expression was calculated relative to *SDHα*. This housekeeping gene was chosen from eight candidate genes based on its expression compared with *Erdr1* and its stability under experimental conditions. For analysis of the whole lung, expression was normalized to the amount of mRNA as measured by the Qubit fluorometer (Invitrogen).

Cloning and manipulation of *Erdr1* expression

Full-length *Erdr1* was cloned from PMC and MEF cDNA and sequenced as described in the Supplementary Experimental Procedures. For expression by lentiviral vectors, *Erdr1* cDNA was cloned into a pLenti7.3 plasmid (Invitrogen) containing either the EF1α or cytomegalovirus (CMV) promoter (see Supplementary Experimental Procedures). Lentiviral vectors were packaged in A293T cells according to the manufacturer's instructions.

Erdr1 expression was inhibited by transducing target cells with short hairpin RNAs (shRNA). Candidate shRNA sequences were confirmed by the University of North Carolina at Chapel Hill Genome Analysis facility. These sequences and a scrambled control sequence were cloned into heparin sulfate proteoglycan (pHSPG) vectors (see Supplementary Experimental Procedures; refs. 22, 23). HSPG viral vectors were packaged as described in the Supplementary Experimental Procedures. PMCs and MEFs were transduced by spin inoculation in 6-well plates with polybrene (4 μg/mL; Sigma) and virus (multiplicity of infection = 5). Transduction efficiency was assessed by measuring the percentage of eGFP positive cells by flow cytometry. Knockdown efficiency was determined by RT-PCR. Of the candidate sequences tested, two were chosen for this study based on the degree of *Erdr1* inhibition.

Overexpression of *Erdr1* was accomplished using the GeneSwitch vector system (Invitrogen). After cloning, *Erdr1* and *LacZ* control plasmids were linearized with SapI restriction endonuclease (NEB). One microgram of plasmid DNA was transfected using Qiagen Attractene reagent according to the manufacturer's instructions (Qiagen). After an 8-hour incubation, RU486 (1 μmol/L final concentration) was added to the cells. Seventy-two hours later, expression of *Erdr1* was measured by RT-PCR in an aliquot of these cells. The remainder was injected into mice as described above.

Analysis of CLL samples

Peripheral blood samples were obtained from patients with CLL through UNC's Tissue Procurement Facility. Only patients with more than 95% lymphocytes on their complete blood count differential were included; all patients were consented according to policies of the UNC Institutional Review Board. Peripheral blood monocytes (PBMC) were isolated from EDTA samples using lymphocyte separation medium (MP Biomedicals) according to the manufacturer's instructions. Cells were washed 5 times, resuspended in 10% RPMI, and maintained at 5% CO_2 and 37°C overnight. On the day of collection, 10^4 M2-10B4 cells in 10% DMEM were added to 6-well plates and were treated with 2 μg/mL of mitomycin C (Sigma). The following day, the wells were washed twice with warm PBS and 10^6 PBMCs were added in 10% RPMI.

Ninety-six hours after the initiation of the coculture, peripheral blood cells were harvested and analyzed for apoptosis with Annexin V and PI. M2-10B4 cells were excluded by their eGFP expression.

Statistical analysis

Unless otherwise stated, data are presented as the mean of measurements taken from three or more separate experiments. Statistical error for these means is presented as ±1 SEM. *P* values were determined by the Mann–Whitney test, and *P* values of <0.05 were considered significant. The Bonferroni correction was applied to experiments with more than two experimental groups.

Results

Erdr1 has greater expression in the lungs and PMCs of WT than *Ccr5*$^{-/-}$ mice

We searched for genes that might be critical for the CCR5-dependent promotion of metastasis by comparing mRNA from WT and *Ccr5*$^{-/-}$ mice that were intravenously injected

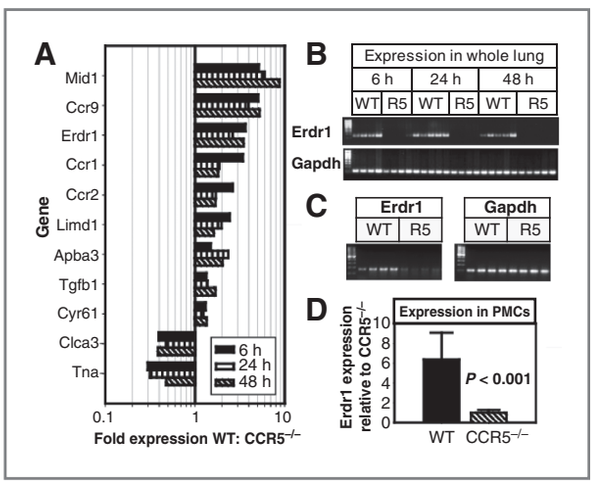

Figure 1. *Erdr1* is upregulated in the lungs and PMCs of WT mice compared with *Ccr5*$^{-/-}$ mice. A, the bar graph shows relative expression of genes from WT mice compared with *Ccr5*$^{-/-}$ mice. Lungs were harvested 6, 24, and 48 hours after intravenous injection of B16-F10 melanoma cells. After mRNA extraction, cDNA was formed and pooled for application to an Affymetrix GeneChip Genome 430 Arrays ($n = 27$). B, semiquantitative RT-PCR for *Erdr1* applied to the unpooled mouse lung samples from the experiment described above. The gel shows detectable *Erdr1* mRNA for each WT mouse. C, semiquantitative PCR as applied to cDNA from four WT and four CCR5$^{-/-}$ mice without tumor injection. D, relative *Erdr1* expression in PMCs of WT and *Ccr5*$^{-/-}$ mice by RT-PCR. Gene expression was standardized to β-actin and then was normalized to *Erdr1* expression in *Ccr5*$^{-/-}$ PMCs ($n = 12$).

Published OnlineFirst November 6, 2013; DOI: 10.1158/1541-7786.MCR-13-0164

with B16-F10 melanoma cells. Analysis revealed 11 candidate genes that were differentially expressed at 6, 12, and 24 hours after injection (Fig. 1A). Semiquantitative RT-PCR was then performed on the unpooled cDNA samples using primers for each of these genes (Supplementary Fig. S1). *Erdr1* expression was detected in 100% of WT mice ($n = 14$); but in 0 ($n = 13$) of the *Ccr5*$^{-/-}$ mice (Fig. 1B). This same pattern was also seen in control mice that did not receive tumor injections (Fig. 1C). The expression patterns for the remaining 10 genes were much more heterogeneous. For example, *Mid1* was detectable in 50% of the WT and 38.5% of the *Ccr5*$^{-/-}$ mice, whereas *Ccr9* was evident in 64.3% of the WT and 46.2% of the *Ccr5*$^{-/-}$ mice. As a result, we chose to further characterize the role of ERDR1 in the promotion of lung metastasis.

Semiquantitative RT-PCR was then performed on the unpooled cDNA samples using primers for each of these genes (Supplementary Fig. S1). *Erdr1* expression was detected in all 14 WT mice; however, expression was near or below the threshold of detection for all 13 *Ccr5*$^{-/-}$ mice (Fig. 1B). This same pattern was also seen in control mice that did not receive tumor injections (Fig. 1C). The expression patterns for the remaining 10 genes were much more heterogeneous. As a result, we chose to further characterize the role of ERDR1 in the promotion of lung metastasis.

We have previously shown metastases can be increased in *Ccr5*$^{-/-}$ mice with the adoptive transfer of WT PMCs but not *Ccr5*$^{-/-}$ PMCs (24). Because this disparity might have been due to the increased expression of *Erdr1* in the WT cells, gene expression was measured in WT and *Ccr5*$^{-/-}$ PMCs using RT-PCR. As was the case for the whole lung, *Erdr1* expression was 6.4 ± 2.7–fold higher in the WT PMCs than in the *Ccr5*$^{-/-}$ cells ($P < 0.001$; Fig. 1D).

Given the limited published data on *Erdr1*, the sequence of the gene expressed by PMCs was compared with that described in the WEHI-3B cell line (13). As shown in Supplementary Fig. S2, the open reading frame in the *Erdr1* consensus sequence was 100% identical to the sequence found in the WEHI-3B cell line.

CCL4 induces the expression of *Erdr1* in CCR5-expressing PMCs

We established an *in vitro* association between ERDR1 and CCR5 by treating PMCs with 50 ng/mL of the Ccr5-specific chemokine Ccl4. As measured by RT-PCR, *Erdr1* expression in WT PMCs was increased by 1.33 ± 0.06–fold ($P < 0.05$) after 24 hours of incubation with Ccl4. By 48 hours, expression had increased by 3.36 ± 0.14–fold ($P < 0.001$; Fig. 2A). Ccl4 did not increase expression of *Erdr1* in *Ccr5*$^{-/-}$ PMCs.

The relationship between ERDR1 and CCL4 was verified by inhibiting the intracellular signaling pathways induced by CCL4. To do so, WT PMCs were treated with the MAP2K inhibitor U0126 or the PI3K inhibitor LY294002. As shown in Fig. 2B, Ccl4 increased expression of *Erdr1* following

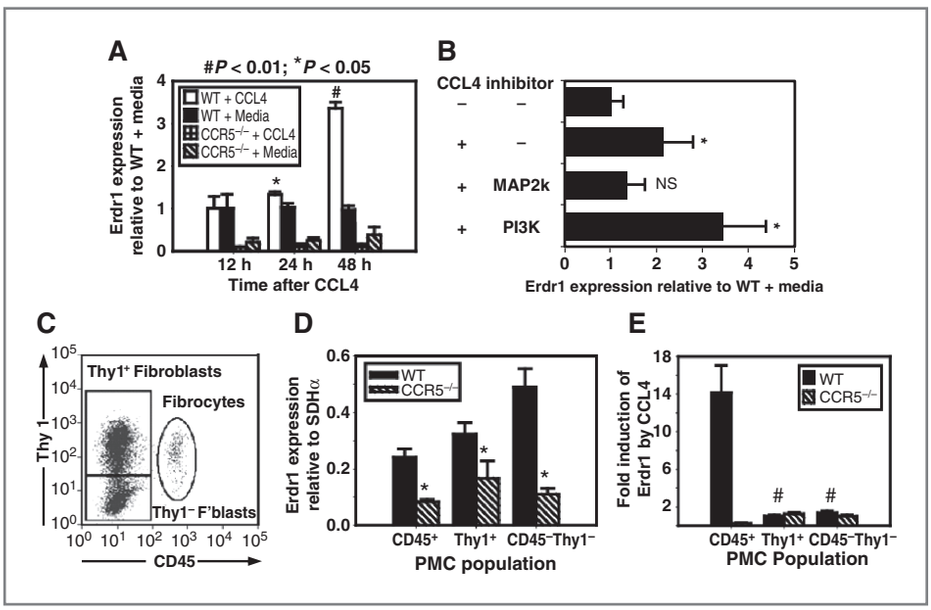

Figure 2. Stimulation of Ccr5 on PMCs induces expression of *Erdr1*. A, *Erdr1* expression by RT-PCR after Ccl4 treatment. WT and *Ccr5*$^{-/-}$ PMCs were stimulated with 50 ng/mL of Ccl4 after overnight culture in serum-free media. mRNA was harvested at 0, 24, and 48 hours. The bar graph shows expression of *Erdr1* normalized to baseline expression in WT PMCs. Significant increases in *Erdr1* expression were detectable in WT PMCs at 24 and 48 hours. No significant changes were noted in *Ccr5*$^{-/-}$ PMCs. B, the response of *Erdr1* to Ccl4 following treatment with 10 μmol/L of the MAP2K inhibitor U0129 and 20 μmol/L of the PI3K inhibitor LY294002. *Erdr1* expression is inhibited by U0129 (third bar) but not LY294002 (fourth bar). C, PMC subpopulations. The dot plot shows flow cytometric analysis of PMC populations as defined by CD45 and Thy-1. D, bar graph showing *Erdr1* expression in PMCs sorted by CD45 and Thy-1. All subpopulations of WT cells expressed more *Erdr1* than *Ccr5*$^{-/-}$ ($P < 0.05$). E, the bar graph shows induction of *Erdr1* after stimulation with Ccl4 in PMC subpopulations. PMCs were sorted 48 hours after treatment with 50 ng/mL of Ccl4. Only WT CD45^{+} PMCs exhibited a significant increase in *Erdr1* expression ($P < 0.01$).

Published OnlineFirst November 6, 2013; DOI: 10.1158/1541-7786.MCR-13-0164

treatment with LY294002 by 3.44 ± 0.92–fold ($P < 0.05$), but not with U0126 (Fig. 2B).

Cultured PMCs contain three different populations of stromal cells, which can be differentiated by their expression of CD45 and Thy-1 (10). Flow cytometric analysis identified fibrocytes as CD45-positive with intermediate expression of Thy-1. Fibroblasts, on the other hand, were $CD45^-$ and could be separated into two additional populations based on Thy-1 expression (Fig. 2C). All three of these WT populations expressed more *Erdr1* than their $Ccr5^{-/-}$ counterparts (Fig. 2D).

Fibrocytes also express more CCR5 than fibroblasts (10). Given this observation, fibrocytes were expected to have a greater response to CCL4 than fibroblasts. This hypothesis was tested by treating PMCs with Ccl4 for 48 hours and then by sorting the cells by Thy-1 and CD45 expression. As predicted, WT $CD45^+$ fibrocytes increased their expression of *Erdr1* by 14.2 ± 2.9–fold. *Erdr1* expression was not induced in the $Ccr5^{-/-}$ fibrocytes or fibroblasts ($P < 0.01$; Fig. 2E).

Experimental pulmonary metastasis is reduced after knockdown of *Erdr1*

The effect of ERDR1 on metastasis was directly tested by manipulating the amount of ERDR1 expressed by stromal cells within the lung before injection with B16-F10 cells. In the first series of experiments, metastasis was measured in $Ccr5^{-/-}$ mice injected with *Erdr1* knockdown or control stromal cells. To this end, we selected two HSPG retroviral vectors carrying different *Erdr1*-specific shRNA sequences and one vector carrying scrambled shRNA control sequence (Supplementary Fig. S3A).

This strategy was applied to MEFs rather than PMCs for several reasons. First, MEFs expressed greater amounts of *Erdr1* than PMCs (Supplementary Fig. S3B). As a result, shRNA treatment would generate a greater difference in *Erdr1* expression and amplify effects of the gene on metastasis. Second, PMCs transduced with *Erdr1* shRNAs expanded poorly (Supplementary Fig. S3C). This constraint limited the technical feasibility of these experiments and raised questions about the persistence of the knockdown cells *in vivo*. Despite these differences, unmanipulated WT MEFs did promote metastasis in $Ccr5^{-/-}$ mice similar to that found by injecting WT PMCs (Supplementary Fig. S3D). Transduction of MEFs also produced viable cells with a mean reduction in *Erdr1* expression of 55% ± 1.0% for shRNA #1 and 70% ± 6.5% for shRNA #2 (Fig. 3A).

Compared with the control MEFs, *Erdr1* knockdown MEFs were associated with a 32.7% and 32.4% reduction in lung metastasis ($P < 0.05$; Fig. 3B and C). This result suggested that ERDR1 acts to promote metastasis or inhibition of ERDR1 reduces metastasis. The latter was ruled out by transferring *Erdr1* knockdown MEFs into WT mice. There were no measurable differences in metastasis when

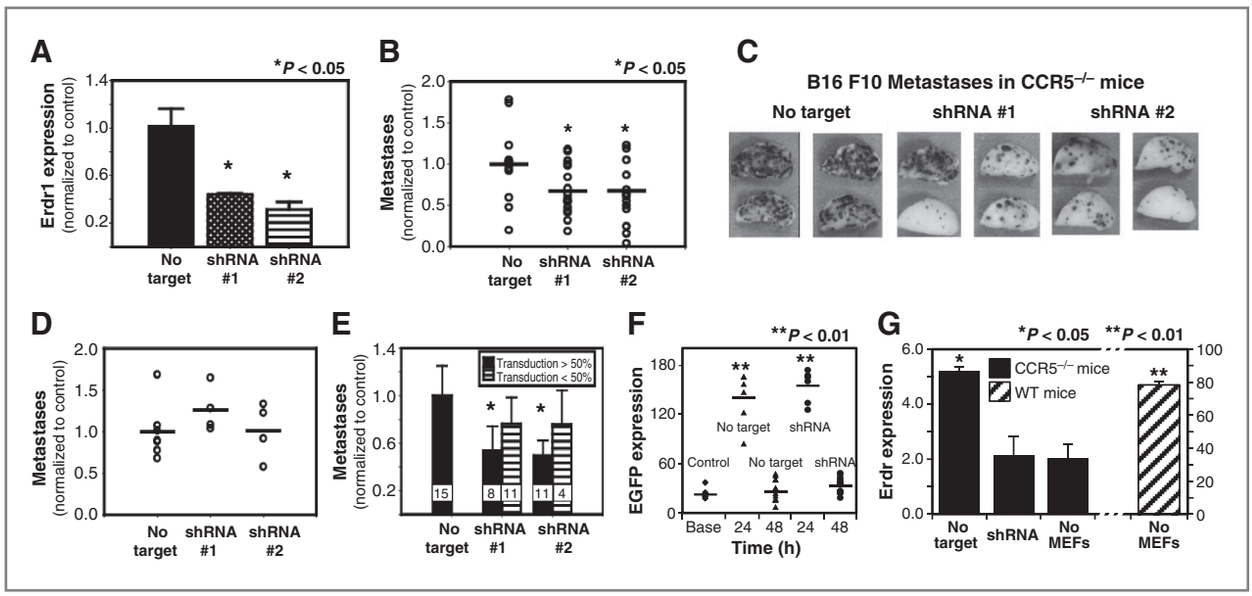

Figure 3. Inhibition of *Erdr1* inhibits metastasis. A, RT-PCR measurement of *Erdr1* expression in MEFs 48 hours after transduction with shRNA retroviral constructs. Results normalized to MEFs transduced with control plasmid. B, graph showing the number of B16-F10 metastases in $Ccr5^{-/-}$ mice injected with MEFs transduced with control (left), shRNA#1 (middle), or shRNA#2 (right). Mice were injected with 4×10^5 MEFs 24 hours before injection with 7.5×10^5 melanoma cells. Metastases are normalized to mice treated with control MEFs; results are pooled from three different experiments. C, photographs of the lungs (left upper lobe) of representative mice described in B. D, graph showing metastases in WT mice injected with control- or shRNA-transduced MEFs. Results normalized to the control MEF group. E, bar graph representing the number of B16-F10 metastases in $Ccr5^{-/-}$ mice. Black bars represent mice that received more than 50% transduced MEFs; striped bars are mice that received less than 50% transduced MEFs. The sample sizes are given just above the *x*-axis. F, the graph shows the amount of eGFP detected from the lung of $Ccr5^{-/-}$ injected with MEFs that had been transduced with control or shRNA plasmids. eGFP was detected by ELISA. The first column on the left is eGFP expression in mice injected with unmanipulated MEFs. G, RT-PCR measurement of *Erdr1* in the lung of $Ccr5^{-/-}$ mice 24 hours after injection with 4×10^5 MEFs transduced with control or shRNA. Columns on the right show *Erdr1* expression of $Ccr5^{-/-}$ and WT mice without MEF injection.

Published OnlineFirst November 6, 2013; DOI: 10.1158/1541-7786.MCR-13-0164

comparing shRNA knockdown MEFs with control-transduced MEFs (Fig. 3D).

The transduction efficiency varied from experiment to experiment. This observation prompted the comparison of mice that received greater than 50% transduced MEFs with those that received less than 50%. *Ccr5*$^{-/-}$ mice that received greater than 50% shRNA-transduced MEFs had significantly fewer metastases (shRNA#1 = 53.3%; shRNA#2 = 50.4%) than those that received less than 50% transduced cells (shRNA#1 = 23.8%; shRNA#2 = 15.4%; Fig. 3E). Thus, a greater number of shRNA-transduced MEFs were associated with fewer metastases.

Our observation that inhibition of ERDR1 inhibits metastasis could also be explained by differences in the survival of the injected MEFs. The number of viable MEFs expressing eGFP in the lung was determined by measuring eGFP in the lung by ELISA. This assay revealed no differences in the lungs from animals injected with control- or *Erdr1* shRNA–transduced MEFs. Animals receiving transduced MEFs had significantly more eGFP than animals injected with unmanipulated MEFs at 24 hours ($P < 0.01$). Differences in eGFP amount were lost at 48 hours (Fig. 3F). Our technique was further confirmed by measuring *Erdr1* expression in the lungs of *Ccr5*$^{-/-}$ mice after injection with shRNA or controlled transduced MEFs. Twenty-four hours after injection with 4×10^5 control MEFs, *Erdr1* expression was increased by 2.5 ± 0.8–fold over shRNA-transduced MEFs (Fig. 3G).

ERDR1 promotes survival of chronic lymphocytic leukemia cells

The ability of ERDR1 to promote experimental metastasis is not well explained by its principal function of hemoglobinization. Other functions have not been well described. Our experience with MEFs suggested that ERDR1 could oppose apoptosis. Though no differences in apoptosis were noted at baseline, ERDR1 countered apoptosis when cells were challenged with staurosporine, an apoptotic stimulus. In these experiments, *Erdr1* knockdown by shRNA #1 and #2 was associated with a greater percentage of apoptotic cells than control transduction (32.7% ± 1.8% vs. 40.2% ± 1.7% vs. 48.1% ± 2.1%, $P < 0.05$). These differences in apoptosis were lost when these cells were treated with the pan-caspase inhibitor Z-VAD (Fig. 4A).

The effect of ERDR1 on apoptosis was also tested by coculturing primary CLL cells with M2-10B4 stromal cells. Without stromal cell support, CLL cells undergo apoptosis within 48 to 72 hours. Therefore, the contribution of ERDR1 to this process could be examined by comparing CLL cell survival using stromal cells treated with *Erdr1*shRNAs. Accordingly, we selected stable control and knockdown clones based on similarities in

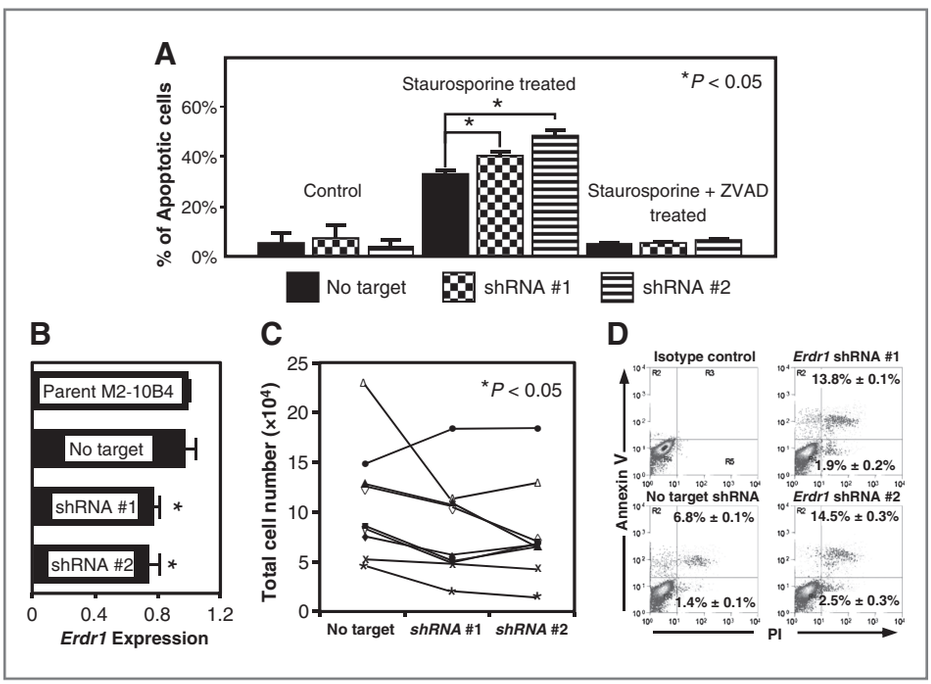

Figure 4. Inhibition of *Erdr1* promotes apoptosis of primary chronic lymphocytic leukemia cells. A, effect of *Erdr1* knockdown on staurosporine-induced apoptosis. MEFs were transduced with *Erdr1* knockdown or control shRNA and were treated with or without staurosporine (100 nmol/L). The bar graph shows a disproportionate increase the apoptosis of MEFs treated with *Erdr1* shRNA. The differences between control- and knockdown shRNA–transduced cells were lost when the caspase inhibitor Z-VAD-FMK was added. B, *Erdr1* expression in M2-10B4 cell lines. Results are expressed relative to the parent line (top). The bottom three lines are stable clones transduced with nontarget control, shRNA#1, or shRNA#2 plasmids. C, Total cell number of CLL cells cocultured with M2-10B4 clones. Each line represents a sample from an individual patient. The points on the left are the cell number after culture with nontargeted control M2-10B4 cells. The points in the center and right are numbers after culture with shRNA knockdown lines. Cells were harvested after 96 hours of culture. D, representative sample dot plots of CLL samples cocultured with M2-10B4 clones. The mean ± SEM is given for all 10 CLL samples.

Published OnlineFirst November 6, 2013; DOI: 10.1158/1541-7786.MCR-13-0164

proliferation and on expression of *Erdr1*. Compared with the nontargeted line, the *Erdr1* expression was 76.8% ± 3.3% for shRNA #1 and 74.0% ± 6.5% for shRNA #2 ($P < 0.05$; Fig. 4B).

At 96 hours, the cell counts were higher when the CLL cells were cocultured with control cell lines compared with *Erdr1* knockdown lines [odds ratio (OR), 1.88 ± 0.27, 2.52 ± 0.66 respectively, $P < 0.05$; Fig. 4C]. This increase in the total cell number was associated with a decrease in the percentage of apoptotic cells (OR, 0.69 ± 0.18, 0.58 ± 0.12, respectively; Fig. 4D).

Discussion

Therapeutic strategies that disrupt the tumor stroma have been limited by the lack of suitable targets. Our group searched for such a target by comparing the gene expression from the lungs of WT and *Ccr5*$^{-/-}$ mice because Ccr5 signaling by the host stromal cells promotes metastasis (24). This search identified *Erdr1* as overexpressed in the lungs of WT compared with *Ccr5*$^{-/-}$ mice injected with tumor cells. Though previously associated with the bone marrow stroma, the expression of this gene in the lung stroma was established by detecting it in PMCs, which are made up of both fibroblasts and fibrocytes. The reintroduction of ERDR1 into *Ccr5*$^{-/-}$ mice by the adoptive transfer of MEFs restored the prometastatic stroma. Furthermore, we found that ERDR1 inhibited apoptosis of human CLL cells. Therefore, we propose that ERDR1 expression by stromal cells promotes invasion and survival of cancer cells by inhibiting apoptosis of these cells.

We chose to study *Erdr1* because it was one of 11 genes that were differentially expressed in the lung during the first 48 hours of tumor growth. Several of these 11 genes have already been associated with cancer progression. For example, Cyr61 has been associated with poor prognosis in squamous cell cancers of the head and neck (25) and esophagus (26). CCR2 has been linked to breast cancer metastasis (27). The inclusion of genes with known tumor-promoting properties substantiates the robustness of our approach. Nevertheless, of these 11 genes, only *Erdr1* demonstrated differential expression in all 27 mice tested.

The identification of ERDR1 was somewhat unexpected because previous work had focused on its role in hemoglobin synthesis. However, a broader physiologic role for this gene is implied by its expression in a wide variety of developing and mature tissues. In addition to the bone marrow (13), gene expression has been demonstrated in the mammary gland, spleen, and lymph node (28). Others have found *Erdr1* expression during retinal development (29), gonadal differentiation (18), liver development (30), and placental morphogenesis (31). The expression of *Erdr1* during development is noteworthy, because it suggests a potential role in malignancy. Cancer gene expression often recapitulates tissue-specific development programs (32, 33). Consequently, developmental genes are candidate oncogenes. In this context, the contribution of ERDR1 to cancer cell survival may not be surprising.

These data provide an additional mechanism by which CCR5 promotes cancer progression, namely by the induction of *Erdr1*. The capacity of Ccr5 to increase *Erdr1* expression was demonstrated in PMCs following treatment with Ccl4, a ligand with specificity for Ccr5. This expression was the greatest in the migrating fibrocyte population, which was expected given their increased expression of Ccr5. This observation is notable because fibrocytes have the greater effect on metastasis than either Thy-1^{+} or Thy-1^{-} fibroblasts (10).

The role of ERDR1 in cancer progression is complex. Jung and colleagues have shown that recombinant ERDR1 suppresses the invasion of human gastric cancer cells (34). This observation follows reports that ERDR1 inhibits metastasis of melanoma cells (35). Our data can be harmonized with these apparently contradictory studies by noting major differences in the experimental methods. Our studies were conducted in *Ccr5*$^{-/-}$ mice that have a low basal expression of *Erdr1*. Furthermore, *Erdr1* expression was manipulated through bystander cells rather than within the cancer cell. Therefore, our experiments highlight the effect of ERDR1 on the surrounding stroma whereas the preceding references focus on the effect of ERDR1 on the cancer cells.

The prometastatic and antimetastatic properties of ERDR1 attest to the bimodal response induced by ERDR1 (14). When the baseline expression of *Erdr1* is reduced, induction of the gene likely promotes cell survival by inhibiting apoptosis. This phenomenon was observed during treatment with staurosporine, and is similar to our CLL data. This relationship is also substantiated by the observation that apoptosis of melanoma cells is increased in the *Ccr5*$^{-/-}$ mouse (12). An inverse relationship between *Erdr1* expression and apoptosis has also been demonstrated in a Nox2$^{-/-}$ mouse undergoing reperfusion injury (36). This model is consistent with our data showing inhibition of *Erdr1* inhibits metastasis. However, when the transcription of *Erdr1* reaches a threshold, apoptosis increases and cell viability diminishes. This phenomenon has been demonstrated in keratinocytes that are undergoing ultraviolet B treatment (35).

Our experiments looked at the effects of ERDR1 as it was expressed by several cell types, including PMCs, MEFs, and M2-10B4 cells. We have seen similar results when comparing PMCs and fibrocytes from WT and *Ccr5*$^{-/-}$ mice (37). Like our genetically manipulated cells, cells from these animals differentially express *Erdr1*. In all of these experiments, greater expression of *Erdr1* in the transferred cells led to a greater tumor burden for the recipient.

CCR5 expression can have diverse implications for cancer prognosis depending on the tissues that express it. In mouse models, Ccr5 boosts CD4^{+}-dependent, CD8^{+} T-cell responses (38), although it may also lower infiltration by those T cells (12). Patients with CCR5^{+}-infiltrating lymphocytes had a better outcome in colorectal cancer (39, 40) or when undergoing immunotherapy for melanoma (41). On the other hand, expression by the tumor tissue is considered a poor marker in melanoma (42), prostate cancer

Published OnlineFirst November 6, 2013; DOI: 10.1158/1541-7786.MCR-13-0164

(43), and breast cancer (44, 45). CCR5 expression on osteosarcoma cells upregulates integrins and predisposes them to metastasis (46). Expression of Ccr5 by the tumor fibroblasts has been associated with the promotion of pulmonary metastasis in murine models (11, 24) and the progression of lung cancer in patients (47). Targeting ERDR1 may be more advantageous than targeting CCR5 because it may inhibit progression mediated by the stroma without inhibiting the antitumor immune response.

The study of ERDR1 in human disease is complicated by the lack of a known human homolog. Nevertheless, the gene has been sequenced from human tissues by several laboratories. ERDR1 has been detected in human keratinocytes (48), lymphoma (13), and HEK293 cells (15). Our laboratory has also detected *ERDR1* in nurse-like cells (49). All of these investigators have found near sequence identity between the human and murine genes.

In summary, this article identifies ERDR1 as a stromal-derived cytokine that promotes cancer progression. Furthermore, it establishes an additional means by which inflammatory chemokines contribute to cancer progression. The relationship between ERDR1 and CCR5 is clinically significant because CCR5 inhibitors are already in clinical trials (50). Further understanding of this interaction may provide a means of separating the beneficial antitumor immune responses from the harmful protumor stromal support. Finally, our data suggest that this relatively unknown gene may be critical to understanding and manipulating tumor–stroma interactions.

Disclosure of Potential Conflicts of Interest

No potential conflicts of interest were disclosed.

Authors' Contributions

Conception and design: R.L Mango, J.S. Serody, H.W. van Deventer
Development of methodology: R.L Mango, Q.P. Wu, H.W. van Deventer
Acquisition of data (provided animals, acquired and managed patients, provided facilities, etc.): R.L Mango, Q.P. Wu, M. West, E.C. McCook, J.S. Serody, H.W. van Deventer
Analysis and interpretation of data (e.g., statistical analysis, biostatistics, computational analysis): R.L Mango, J.S. Serody, H.W. van Deventer
Writing, review, and/or revision of the manuscript: R.L Mango, J.S. Serody, H.W. van Deventer
Administrative, technical, or material support (i.e., reporting or organizing data, constructing databases): R.L Mango, Q.P. Wu
Study supervision: Q.P. Wu, J.S. Serody, H.W. van Deventer

Acknowledgments

The authors thank Peter Dormer for initial assistance in obtaining antibody for Western blots, and Deborah Taxman for advice on constructing shRNA vectors.

Grant Support

This work was supported by NIH grant P50CA058223 (J.S. Serody) and ACS grant RSG 118750 (H.W. van Deventer). R.L Mango is a member of the Medical Scientist Training Program T32 GM008719.

The costs of publication of this article were defrayed in part by the payment of page charges. This article must therefore be hereby marked *advertisement* in accordance with 18 U.S.C. Section 1734 solely to indicate this fact.

Received April 3, 2013; revised August 29, 2013; accepted September 7, 2013; published OnlineFirst November 6, 2013.

References

1. Zhou Y, You MJ, Young KH, Lin P, Lu G, Medeiros LJ, et al. Advances in the molecular pathobiology of B-lymphoblastic leukemia. Hum Pathol 2012;43:1347–62.
2. Rasanen K, Vaheri A. Activation of fibroblasts in cancer stroma. Exp Cell Res 2010;316:2713–22.
3. Grivennikov SI, Greten FR, Karin M. Immunity, inflammation, and cancer. Cell 2010;140:883–99.
4. Zhang J, Liu J. Tumor stroma as targets for cancer therapy. Pharmacol Therapeut 2013;137:200–15.
5. Steller EJ, Raats DA, Koster J, Rutten B, Govaert KM, Emmink BL, et al. PDGFRB promotes liver metastasis formation of mesenchymal-like colorectal tumor cells. Neoplasia 2013;15:204–17.
6. Hiratsuka S, Nakamura K, Iwai S, Murakami M, Itoh T, Kijima H, et al. MMP9 induction by vascular endothelial growth factor receptor-1 is involved in lung-specific metastasis. Cancer Cell 2002;2:289–300.
7. Studebaker AW, Storci G, Werbeck JL, Sansone P, Sasser AK, Tavolari S, et al. Fibroblasts isolated from common sites of breast cancer metastasis enhance cancer cell growth rates and invasiveness in an interleukin-6-dependent manner. Cancer Res 2008;68:9087–95.
8. Cabezón T, Skibshøj I, Klingelhöfer J, Grigorian M, Gromov P, Rank F, et al. Expression of S100A4 by a variety of cell types present in the tumor microenvironment of human breast cancer. Int J Cancer 2007;121:1433–44.
9. Saha A, Lee YC, Zhang Z, Chandra G, Su SB, Mukherjee AB. Lack of an endogenous anti-inflammatory protein in mice enhances colonization of B16F10 melanoma cells in the lungs. J Biol Chem 2010;285:10822–31.
10. van Deventer HW, Wu QP, Bergstralh DT, Davis BK, O'Connor BP, Ting JP, et al. C-C chemokine receptor 5 on pulmonary fibrocytes facilitates migration and promotes metastasis via matrix metalloproteinase 9. Am J Pathol 2008;173:253–64.
11. Wu Y, Li Y-Y, Matsushima K, Baba T, Mukaida N. CCL3-CCR5 axis regulates intratumoral accumulation of leukocytes and fibroblasts and promotes angiogenesis in murine lung metastasis process. J Immunol 2008;181:6384–93.
12. Song JK, Park MH, Choi DY, Yoo HS, Han SB, Yoon do Y, et al. Deficiency of C-C chemokine receptor 5 suppresses tumor development via inactivation of NF-kappaB and upregulation of IL-1Ra in melanoma model. PLoS One 2012;7:e33747.
13. Dormer P, Spitzer E, Frankenberger M, Kremmer E. Erythroid differentiation regulator (EDR), a novel, highly conserved factor I. Induction of haemoglobin synthesis in erythroleukaemic cells. Cytokine 2004;26:231–42.
14. Dormer P, Spitzer E, Moller W. EDR is a stress-related survival factor from stroma and other tissues acting on early haematopoietic progenitors (E-Mix). Cytokine 2004;27:47–57.
15. Gillingwater TH, Wishart TM, Chen PE, Haley JE, Robertson K, MacDonald SH-F, et al. The neuroprotective WldS gene regulates expression of PTTG1 and erythroid differentiation regulator 1-like gene in mice and human cells. Hum Mol Genet 2006;15:625–35.
16. Lee JH, Kim CH, Kim DG, Ahn YS. Microarray analysis of differentially expressed genes in the brains of tubby mice. Korean J Physiol Pharmacol 2009;13:91–7.
17. Brown AR, Rebus S, McKimmie CS, Robertson K, Williams A, Fazakerley JK. Gene expression profiling of the preclinical scrapie-infected hippocampus. Biochem Bioph Res Co 2005;334:86–95.
18. Nef S, Schaad O, Stallings NR, Cederroth CR, Pitetti JL, Schaer G, et al. Gene expression during sex determination reveals a robust female genetic program at the onset of ovarian development. Dev Biol 2005;287:361–77.
19. Anderson KC. Targeted therapy of multiple myeloma based upon tumor-microenvironmental interactions. Exp Hematol 2007;35:155–62.
20. Andres PG, Beck PL, Mizoguchi E, Mizoguchi A, Bhan AK, Dawson T, et al. Mice with a selective deletion of the CC chemokine receptors 5 or

Published OnlineFirst November 6, 2013; DOI: 10.1158/1541-7786.MCR-13-0164

2 are protected from dextran sodium sulfate-mediated colitis: Lack of CC chemokine receptor 5 expression results in a NK1.1+ lymphocyte-associated Th2-type immune response in the intestine. J Immunol 2000;164:6303–12.
21. Sipkins DA, Wei X, Wu JW, Runnels JM, Cote D, Means TK, et al. In vivo imaging of specialized bone marrow endothelial microdomains for tumour engraftment. Nature 2005;435:969–73.
22. Coffield VM, Jiang Q, Su L. A genetic approach to inactivating chemokine receptors using a modified viral protein. Nat Biotechnol 2003;21:1321–7.
23. Taxman DJ, Livingstone LR, Zhang J, Conti BJ, Iocca HA, Williams KL, et al. Criteria for effective design, construction, and gene knockdown by shRNA vectors. BMC Biotechnol 2006;6:7.
24. van Deventer HW, O'Connor W Jr, Brickey WJ, Aris RM, Ting JP, Serody JS. C-C chemokine receptor 5 on stromal cells promotes pulmonary metastasis. Cancer Res 2005;65:3374–9.
25. Kok SH, Chang HH, Tsai JY, Hung HC, Lin CY, Chiang CP, et al. Expression of Cyr61 (CCN1) in human oral squamous cell carcinoma: an independent marker for poor prognosis. Head Neck 2010;32:1665–73.
26. Yang Z, Lei Z, Li B, Zhou Y, Zhang G-M, et al. Rapamycin inhibits lung metastasis of B16 melanoma cells through down-regulating alphav integrin expression and up-regulating apoptosis signaling. Cancer Sci 2009;101:494–500.
27. Lu Y, Chen Q, Corey E, Xie W, Fan J, Mizokami A, et al. Activation of MCP-1/CCR2 axis promotes prostate cancer growth in bone. Clin Exp Metastas 2009;26:161–9.
28. Lattin JE, Schroder K, Su AI, Walker JR, Zhang J, Wiltshire T, et al. Expression analysis of G protein-coupled receptors in mouse macrophages. Immunome Res 2008;4:5.
29. Blackshaw S, Harpavat S, Trimarchi J, Cai L, Huang H, Kuo WP, et al. Genomic analysis of mouse retinal development. PLoS Biol 2004;2:e247.
30. Otu HH, Naxerova K, Ho K, Can H, Nesbitt N, Libermann TA, et al. Restoration of liver mass after injury requires proliferative and not embryonic transcriptional patterns. J Biol Chem 2007;282:11197–204.
31. Sferruzzi-Perri AN, Macpherson AM, Roberts CT, Robertson SA. Csf2 null mutation alters placental gene expression and trophoblast glycogen cell and giant cell abundance in mice. Biol Reprod 2009;81:207–21.
32. Kho AT, Zhao Q, Cai Z, Butte AJ, Kim JY, Pomeroy SL, et al. Conserved mechanisms across development and tumorigenesis revealed by a mouse development perspective of human cancers. Genes Dev 2004;18:629–40.
33. Liu H, Kho AT, Kohane IS, Sun Y. Predicting survival within the lung cancer histopathological hierarchy using a multi-scale genomic model of development. PLoS Med 2006;3:e232.
34. Jung MK, Houh YK, Ha S, Yang Y, Kim D, Kim TS, et al. Recombinant ERDR1 suppresses the migration and invasion ability of human gastric cancer cells, SNU-216, through the JNK pathway. Immunol Lett 2013;150:145–51.
35. Jung MK, Park Y, Song SB, Cheon SY, Park S, Houh Y, et al. Erythroid differentiation regulator 1, an interleukin 18-regulated gene, acts as a metastasis suppressor in melanoma. J Invest Dermatol 2011;131:2096–104.
36. Thirunavukkarasu M, Adluri R, Juhasz B, Samuel S, Zhan L, Kaur A, et al. Novel role of NADPH oxidase in ischemic myocardium: a study with Nox2 knockout mice. Funct Integr Genomics 2012;12:501–14.
37. van Deventer HW, Palmieri D A, Wu Q P, McCook E C, Serody J S. Circulating fibrocytes prepare the lung for cancer metastasis by recruiting Ly-6c+ monocytes via CCL2. J Immunol 2013;190:4861–7.
38. González-Martín A, Gómez L, Lustgarten J, Mira E, Mañes S. Maximal T cell–mediated antitumor responses rely upon CCR5 expression in both $CD4^+$ and $CD8^+$ T cells. Cancer Res 2011;71:5455–66.
39. Musha H, Ohtani H, Mizoi T, Kinouchi M, Nakayama T, Shiiba K, et al. Selective infiltration of CCR5(+)CXCR3(+) T lymphocytes in human colorectal carcinoma. Int J Cancer 2005;116:949–56.
40. Schimanski CC, Moehler M, Gockel I, Zimmermann T, Lang H, Galle PR, et al. Expression of chemokine receptor CCR5 correlates with the presence of hepatic molecular metastases in K-ras positive human colorectal cancer. J Cancer Res Clin Oncol 2011;137:1139–45.
41. Petrulio C, Kim-Schulze S, Deraffele G, Morozowiecz D, Mitcham J, Schrama D, et al. P239: CCR5 polymorphism as a predictor of clinical response to high-dose IL-2 therapy in melanoma and renal cell carcinoma. J Surg Res 2007;137:327.
42. Gan Y, Reilkoff R, Peng X, Russell T, Chen Q, Mathai SK, et al. Role of semaphorin 7a signaling in transforming growth factor β1–induced lung fibrosis and scleroderma-related interstitial lung disease. Arth Rheum 2011;63:2484–94.
43. Vaday GG, Peehl DM, Kadam PA, Lawrence DM. Expression of CCL5 (RANTES) and CCR5 in prostate cancer. Prostate 2006;66:124–34.
44. Velasco-Velázquez M, Jiao X, De La Fuente M, Pestell TG, Ertel A, Lisanti MP, et al. CCR5 antagonist blocks metastasis of basal breast cancer cells. Can Res 2012;72:3839–50.
45. Karnoub AE, Dash AB, Vo AP, Sullivan A, Brooks MW, Bell GW, et al. Mesenchymal stem cells within tumour stroma promote breast cancer metastasis. Nature 2007;449:557–63.
46. Wang SW, Wu HH, Liu SC, Wang PC, Ou WC, Chou WY, et al. CCL5 and CCR5 interaction promotes cell motility in human osteosarcoma. PLoS One 2012;7:e35101.
47. Borczuk AC, Papanikolaou N, Toonkel RL, Sole M, Gorenstein LA, Ginsburg ME, et al. Lung adenocarcinoma invasion in TGFbetaRII-deficient cells is mediated by CCL5/RANTES. Oncogene 2008;27:557–64.
48. Kim HJ, Song SB, Yang Y, Eun YS, Cho BK, Park HJ, et al. Erythroid differentiation regulator 1 (ERDR1) is a proapoptotic factor in human keratinocytes. Exp Dermatol 2011;20:920–5.
49. van Deventer HW, Hoffert T, West M, Mango R, Wu QP, Serody J. Bone marrow stromal cells inhibit apoptosis in chronic lymphocytic leukemia cells by expressing erythroid differentiation regulator 1. Blood 2011;118. Abstract nr 1764.
50. Dorr P, Westby M, Dobbs S, Griffin P, Irvine B, Macartney M, et al. Maraviroc (UK-427,857), a potent, orally bioavailable, and selective small-molecule inhibitor of chemokine receptor CCR5 with broad-spectrum anti-human immunodeficiency virus type 1 activity. Antimicrob Agents Chemother 2005;49:4721–32.

AACR American Association for Cancer Research

Molecular Cancer Research

C-C Chemokine Receptor 5 on Pulmonary Mesenchymal Cells Promotes Experimental Metastasis via the Induction of Erythroid Differentiation Regulator 1

Robert L. Mango, Qing Ping Wu, Michelle West, et al.

Mol Cancer Res 2014;12:274-282. Published OnlineFirst November 6, 2013.